reverse mode is favored by depolarization (Eq. 2), this would have resulted as observed, in a much larger Ca^{2+} influx (unidirectional) during depolarizing pulses.

The working scheme (*14*) predicts that the slope of the linear relationship between $[Ca^{2+}]_i$ and current will depend exponentially on voltage as a result of translocation of one positive charge with each ion exchange reaction. The exponential equation that best fits the data (Fig. 3C) indicates a partition parameter r of 0.45, which is similar to the value of 0.35 obtained by measuring putative Na-Ca exchange currents in these cells (*5*).

REFERENCES AND NOTES

1. S. S. Sheu and M. P. Blaustein, in *The Heart and Cardiovascular System*, H. Fozzard *et al.*, Eds. (Raven, New York, 1986), pp. 509–535; L. J. Mullins, *Electrogenic Transport: Fundamental Principles and Physiological Implications*, M. P. Blaustein and M. Lieberman, Eds. (Raven, New York, 1984), pp. 161–179; G. A. Langer, *Annu. Rev. Physiol.* **44**, 435 (1982); D. A. Eisner and W. J. Lederer, *Am. J. Physiol.* **248**, C189 (1985).
2. H. Reuter and H. Seitz, *J. Physiol. (London)* **195**, 451 (1968); D. Mentrard, G. Vassort, R. Fischmeister, *J. Gen. Physiol.* **84**, 201 (1984); D. M. Brill, H. A. Fozzard, J. C. Makielski, J. A. Wasserstrom, *J. Physiol. (London)* **384**, 355 (1987).
3. J. P. Reeves and J. L. Sutko, *J. Biol. Chem.* **258**, 3178 (1983); K. D. Philipson and A. Y. Nishimoto, *ibid.* **257**, 5111 (1982).
4. J. R. Hume and A. Uehara, *J. Gen. Physiol.* **87**, 857 (1986); *ibid.*, p. 883.
5. J. Kimura, A. Noma, H. Irisawa, *Nature (London)* **319**, 596 (1986); J. Kimura, S. Miyame, A. Noma, *J. Physiol. (London)* **384**, 199 (1987).
6. W. G. Wier, A. A. Kort, M. D. Stern, E. G. Lakatta, E. Marban, *Proc. Natl. Acad. Sci. U.S.A.* **80**, 367 (1983); C. H. Orchard, D. A. Eisner, D. G. Allen, *Nature (London)* **304**, 735 (1983).
7. W. G. Wier, M. B. Cannell, J. R. Berlin, E. Marban, W. J. Lederer, *Science* **235**, 325 (1987).
8. S. Mechmann and L. Pott, *Nature (London)* **319**, 597 (1986).
9. G. Grynckiewicz, M. Poenie, R. Y. Tsien, *J. Biol. Chem.* **260**, 340 (1985).
10. L. Barcenas-Ruiz and W. G. Wier, *Circ. Res.* **61**, 148 (1987).
11. L. Barcenas-Ruiz, D. J. G. Beuckelmann, W. G. Wier, *J. Physiol. (London)*, in press.
12. E. Marban and W. G. Wier, *Circ. Res.* **56**, 133 (1985); J. L. Kenyon and J. L. Sutko, *J. Gen. Physiol.* **89**, 921 (1987).
13. We could not use inorganic ions that might have blocked T-type channels (*20*) because these ions quench fura-2 fluorescence and block Na-Ca exchange (*5*).
14. L. J. Mullins, *J. Physiol.* 77, 1139 (1981); L. J. Mullins, *Am. J. Physiol.* **236**, C103 (1979); D. DiFrancesco and D. Noble, *Phil. Trans. R. Soc. London* **B307**, 353 (1985).
15. H. Rasgado-Flores and M. P. Blaustein, *Am. J. Physiol.* **252**, C499 (1987); S. S. Sheu and H. A. Fozzard, *J. Gen. Physiol.* **80**, 325 (1985); J. P. Reeves and C. C. Hale, *J. Biol. Chem.* **259**, 7733 (1984); K. Yau and K. Nakatani, *Nature (London)* **311**, 661 (1984).
16. E. A. Johnson and J. M. Kootsey, *J. Membr. Biol.* **86**, 167 (1985).
17. Mathematically, the term "$\exp[-VF(1 - r)/RT]$" in Eq. 1 increases as V becomes more negative, and since current varies linearly with $[Ca^{2+}]_i$ during Ca^{2+} efflux (Fig. 1C), the slope of the relation will be given by the term $k \times \exp[-VF(1 - r)/RT]$ in Eq. 1.
18. D. A. Eisner and R. D. Vaughan-Jones, *Cell Calcium* **4**, 371 (1983).
19. D. Colquhoun, E. Neher, H. Reuter, C. F. Stevens, *Nature (London)* **294**, 752 (1981)
20. B. Nilius, P. Hess, J. Lansman, R. W. Tsien, *ibid.* **316**, 443 (1985); R. Mitra and M. Morad, *Proc. Natl. Acad. Sci. U.S.A.* **83**, 5340 (1986).

21. Supported by NIH grant HL29473. W.G.W. is an Established Investigator of the American Heart Association and its Maryland Affiliate. D.J.B. is supported by the Deutsche Forschungsgemeinschaft (BE 1113-1-1).

6 August 1987; accepted 30 October 1987

Structure of a Psoralen Cross-Linked DNA in Solution by Nuclear Magnetic Resonance

MILAN T. TOMIC, DAVID E. WEMMER, SUNG-HOU KIM*

One- and two-dimensional nuclear magnetic resonance (NMR) methods were used to determine a three-dimensional model of an eight-base-pair DNA fragment (d-GGGTACCC) cross-linked with psoralen in solution. Two-dimensional nuclear Overhauser effect experiments were used to assign the spectrum and estimate distances for 171 proton pairs in the cross-linked DNA. The NMR-derived model shows a 53° bend into the major groove that occurs primarily at the site of drug addition and a 56° unwinding that spans the eight-base-pair duplex.

PSORALENS (FIG. 1A) ARE A CLASS OF furocoumarins (*1*) that are used for treatment of psoriasis and other skin disorders (*2*), and have also been used as probes of nucleic acid structure and function because they covalently cross-link nucleic acids between opposing strands of duplex regions of DNA (*3*). A three-step mechanism of psoralen cross-linking with DNA has been proposed (*4*). The planar psoralen first intercalates into a double helical region, and ultraviolet (UV, 320 to 400 nm) irradiation initially induces a single cyclobutane addition with a pyrimidine base (Fig. 1B). Photochemistry can occur on either the furan (f) or pyrone (p) side. The furan-side monoadduct still absorbs in this wavelength region, so that a second photoaddition can occur with the pyrone side to form the cross-link (Fig. 1C). Thymines are the preferred site for monoadduct formation (*5*), and psoralen cross-linking occurs at 5′-TpA-3′ sites in DNA (*6, 7*). Psoralen addition products are primarily in the cis-syn conformation (*5, 8*), as confirmed by the x-ray structure of a 8-methoxypsoralen monoadduct [8MOP-thymine (*9*)] and by the NMR analysis of the thymine-psoralen-thymine diadduct (*6*). Physical models based on the monoadduct structure led to the proposal that psoralen cross-links cause a sharp kink in the double helical DNA structure and unwinding of the duplex (*10, 11*).

We have used one- and two-dimensional nuclear magnetic resonance (2D NMR) methods, including through-space nuclear Overhauser effect spectroscopy (NOESY), to analyze the solution structure of a self-complementary DNA octanucleotide d-GGGTACCC that has a 5′-TpA site cross-linked with psoralen. Distance information was obtained by peak integration of NOESY cross peaks. Both model-based refinements and distance geometry methods were then used with the NMR data to generate a solution structure of cross-linked DNA.

A stepwise monomer-addition phosphoramidite method was used to synthesize d-

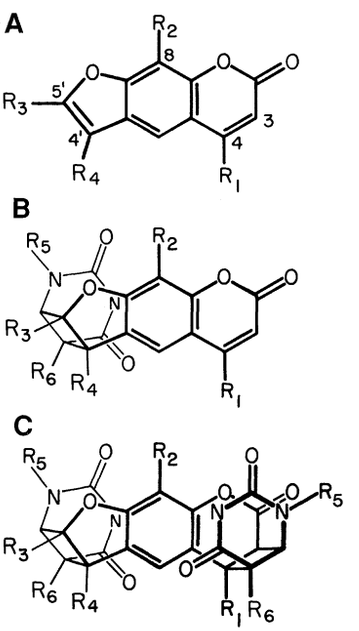

Fig. 1. (**A**) Generalized formula for psoralen; in AMT, R1, R2, and R3 are methyl groups and R4 is CH_2NH_2; in 8-methoxypsoralen (8MOP), R1, R3, and R4 are hydrogens and R2 is OCH_3. (**B**) One of the observed psoralen-thymine monoadduct structures in cis-syn conformation; R5 is deoxyribose sugar and R6 is methyl group of thymine. (**C**) Cross-link of psoralen with thymines; each adduct has the cis-syn configuration.

Department of Chemistry, University of California, Berkeley, CA 94720.

*To whom correspondence should be addressed.

GpGpGpTpApCpCpC (*12*). We used 4′-aminomethyl-4,5′,8-trimethylpsoralen (AMT, Fig. 1A) to obtain a high yield of cross-link (*4*) at the central thymines of the oligomer (*13, 14*). The isolation of a single psoralen cross-link at the 5′-TpA site indicates that this is the preferred site for cross-link formation, although intercalation occurs at all sites.

The 2D NOE spectra of both the unmodified octamer and the purified cross-linked DNA were assigned with the standard sequential method (*15*); the covalently bound psoralen breaks the symmetry of the DNA so that previously equivalent protons on the two strands now have separate resonances (Figs. 2 and 3). Standard sequential connectivities were observed for the unmodified octamer (Fig. 3A) and within each of the four half-strands separated by the drug in the cross-linked oligomer (Fig. 3B). The strand-specific assignment of the symmetric DNA base sequence was resolved by observation of connectivities to the H6 and methyl protons of the modified T residues and to methyl protons on the drug itself. The positions of psoralen methyl groups and the known stereochemistry of the cross-link (*4–6, 8, 9*) were used to unambiguously assign the aromatic protons (Fig. 3, A and B) except for the adenine H2 protons, which were assigned with the nuclear Overhauser effect (NOE) from the imino protons. Sugar protons were assigned by working outward from the aromatic proton to H1′ and H2′, H2″ cross peaks to find the corresponding H3′ and most of the H4′ resonances. The covalent photoaddition of the drug across the C5–C6 double bonds of thymines 4 and 12 shifts the thymine H6 resonances into the same region as the sugar H3′ and H4′ resonances; this was also observed for T-T dimers (*16*). An unusual NOE occurs between the H1′ proton of G11 and the H1′ of T12. The distance between these protons in B-DNA is about 5 Å, whereas in the cross-linked DNA it is ≤3.2 Å. The corresponding peak on the pyrone side, G3 to T4, is not observed, showing that the DNA structure is different on the two sides of the drug. The chemical shifts of the terminal base-pair protons (C1-G16 and G8-C9) are at nearly the same position, indicating that the structural differences of the two sides of the cross-link are limited to three base pairs from the site of addition.

Separate imino resonances are seen for the two halves of the cross-linked octamer (Fig. 4). NOE connectivities were observed from the thymine imino protons to an A H2 proton and to the imino protons of neighboring base pairs, identifying the G3 and G11 imino protons. The G2 and G10 imino protons were not resolved. The G1 and G9 resonances are broad and could not be assigned through NOEs. The T imino resonances in the cross-linked DNA are shifted upfield to approximately 11.7 and 11.2 ppm for T12 and T4, respectively, from their position at 13.4 ppm in native DNA. The octamer NOE connectivities do not provide an absolute assignment of the imino resonances; they were assigned by comparing the asymmetric melting of assigned aromatic resonances (Fig. 5) with that of the imino protons and the H2 protons. Resonances on one side of the DNA duplex began shifting at temperatures 20°C lower than for those on the other side. Similar behavior is also seen for the imino protons (Fig. 4). The difference must arise from asymmetric perturbation of the DNA structure at the psoralen cross-link. The aromatic proton resonances of C14 shift with increasing temperature, beginning at 40°C. Those of C6 on the opposite side of the drug begin to do so at 60°C (Fig. 5). Similar results were seen for C15 versus C7. We assigned the imino protons that broaden first to G1, G2, G3, and T4. We believe that this correlation is sufficiently clear to assign the resonances absolutely.

The larger upfield shift and broadening,

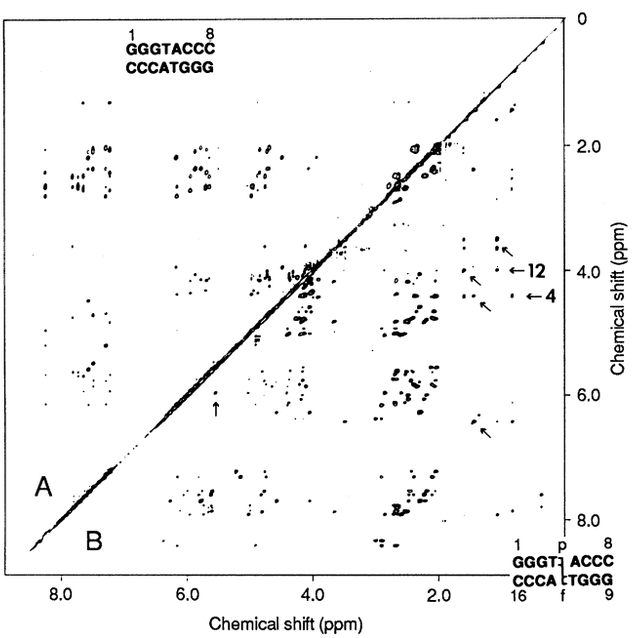

Fig. 2. This figure is divided along the diagonal. (**A**) Upper left; 2D NOE spectrum of d-GGGTACCC (10°C, 100 msec mixing time). (**B**) Lower right; NOE spectrum of psoralen cross-linked octamer (10°C, 200 msec mixing time). Positions of the H6 residues of T4 and T12 are indicated. NOEs between protons on these modified T residues and the psoralen are indicated by diagonal arrows. A vertical arrow indicates the NOE between the H1′ of G11 and the H1′ of T12. Samples contained approximately 1 m*M* DNA in 200 m*M* NaCl, 20 m*M* phosphate buffer, *p*H 7 3-Trimethylsilyl-1-propanesulfonic acid (TSP) was used for internal reference. 2D NOE spectra were collected by the TPPI method (*30*) for quadrature generation in t_1. Spectra were collected on a GE 500-MHz spectrometer in a 5-mm proton probe; ~600 t_1 time points were collected with a delay between experiments of 2.4 seconds and a spectral width of 5682 Hz with 1024 complex points digitized in t_2. All 2D NOE data were processed with the FTNMR program (Hare Research). The data were apodized with a skewed sine function [length 768 data points, phase 45° to 60°, skew 0.5 (*22*), and zero filled to give a final matrix of 1024 by 1024 real data points; t_1 ridges were suppressed by multiplying the first row of the data matrix by 0.5 after the first Fourier transform (*31*).

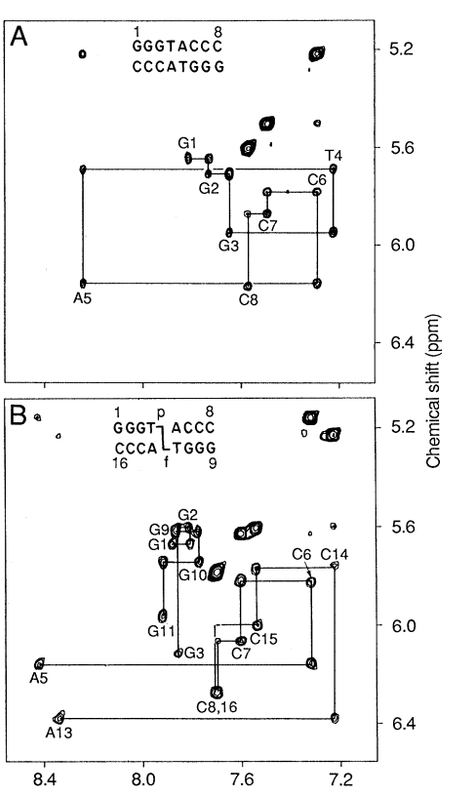

Fig. 3. Expansions of Fig. 2 showing the cross peaks of the aromatic proton to H1′ of the same nucleotide (numbered peaks) and to the H1′ of the sugar of the base on the 5′ side (connected with solid lines). (**A**) Unmodified octamer possessing a center of symmetry with all of the protons sequentially assigned. (**B**) Cross-linked oligomer where the residues on either side of the drug are no longer equivalent. T4 is linked to the pyrone side, and T12 is linked to the furan side of the psoralen.

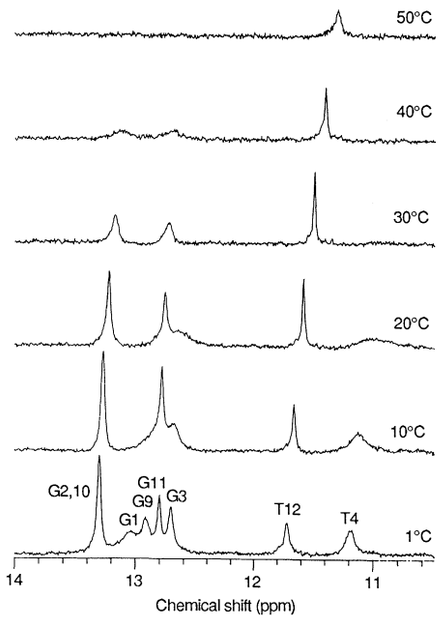

Fig. 4. Imino proton spectra of cross-linked DNA as a function of temperature. Spectra (the solvent contained 10% D_2O for locking) were collected with 1331 pulses (*32*) optimized for excitation of the imino resonances. Baselines in the imino region were flattened with the cubic spline correction provided in the GE software. Residue numbering and buffer are the same as those used in Fig. 2B.

even at 0°C, of the T4 imino proton suggests that it is accessible to solvent and weakly hydrogen bonded. This behavior may be due to the aminomethyl side chain on the furan side of the drug that extends below the plane of the drug and forces the A13 base below it to propeller twist in a direction opposing the bend in the helix, distorting or disrupting the T4-A13 base pairing. In contrast, the T12 imino proton is the last to exchange with solvent, suggesting that the hydrogen bonding with A5 is very stable after cross-linking. Large upfield shifts are observed for T residues that lack the deshielding effect of base pairing (*17*). The upfield shift of the T4 and T12 imino protons may arise primarily from electronic effects, with an additional contribution for T4 from weaker hydrogen bond effects, as observed for T-T dimers (*18*).

The geometry of the psoralen cross-link was derived from crystallographic data on the 8MOP-T monoadduct (*9*), with a second T residue built onto the pyrone side of the psoralen with a cis-syn geometry (*6*). The coordinates from the energy-refined model of the cross-link (*11*) were modified to include the appropriate alterations in sequence and in the substitution on the drug. The positions of methyl groups and the side chain of the AMT were calculated with standard bond lengths and angles from this starting model. Intensities of 2D NOE resonances were determined with the volume integration routine in FTNMR. Distances were determined by comparison of cross peak intensities with those of the resolved cytosine H5 and H6 protons, which were assumed to have a separation of 2.48 Å; 171 independent distances were obtained from NOE spectra taken at mixing times of 50, 100, and 200 msec. For longer distances the longer mixing time points were used. For some poorly resolved resonances, distances were determined by comparison of peak intensities, and correspondingly larger errors were assigned to them. During the refinement (*19*) we included standard hydrogen bonds between both amino and imino protons on all of the G-C base pairs in order to hold the ends of the DNA together in the absence of interstrand NOEs. The imino-proton melting data in Fig. 4 support the assumption that these hydrogen bonds exist. Because of the unusual chemical shifts and melting behavior of the modified T residues, we did not include hydrogen bonds for the A or T residues.

The bent and unwound structure of the AMT cross-linked DNA octamer (obtained after refinement with NMR-derived distances) is shown in Fig. 6. The initial model of the cross-linked DNA was properly base paired and near the B conformation, and was refined to meet the constraints of the distances obtained with NMR (*19*). The structure is consistent with the NOE data, with maximum differences between set constraints and distances in the model of <0.3 Å (with only two interresidue distances violating experimentally determined values by more than 0.2 Å). The protrusion of methyl groups and the aminomethyl side chain from the drug, and the altered geometry of methyls in the photoadducted T residues, cause stacking distortion of the adenine bases flanking the cross-link, which propagates to the neighboring base pairs through steric interactions. However, excluding the bases immediately flanking the drug, the basic stacking of B form DNA is still observed. The two T residues, which are covalently attached to the drug, protrude upwards into the neighboring bases significantly. These constraints result in a 53° bend of the DNA double helical axis into the major groove. In addition, the DNA is unwound by 56° (assuming an average rotation of 36° between base pairs for normal DNA), and there is a displacement of about 1.5 Å of the helix axis by the covalent addition of the drug. These values are in qualitative agreement with those derived from model building (*11*): 45°, 63°, and 1.7 Å for the helix axis kink angle, unwinding angle, and helix axis displacement, respectively, when calculated by the same method of defining helical vectors as used here (*20*). The angle of bend in the helix axis is in qualitative agreement with the observations of Griffith *et al.* (*21*) from electron microscopy.

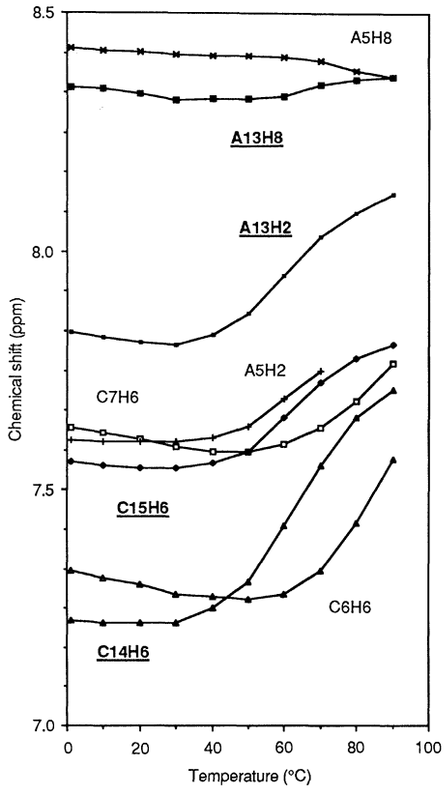

Fig. 5. Plots of aromatic base proton chemical shifts of cross-linked oligomer in D_2O as a function of temperature (residue numbering as in Fig. 2B). The sample was 1 m*M* DNA, 10 m*M* phosphate buffer, *p*H 7. Spectra were obtained with a spectral width of 5682 Hz, with 4096 complex data points, a 70° observe pulse of 8 μsec, a delay of 2.5 seconds between pulses, and 64 scans per spectrum.

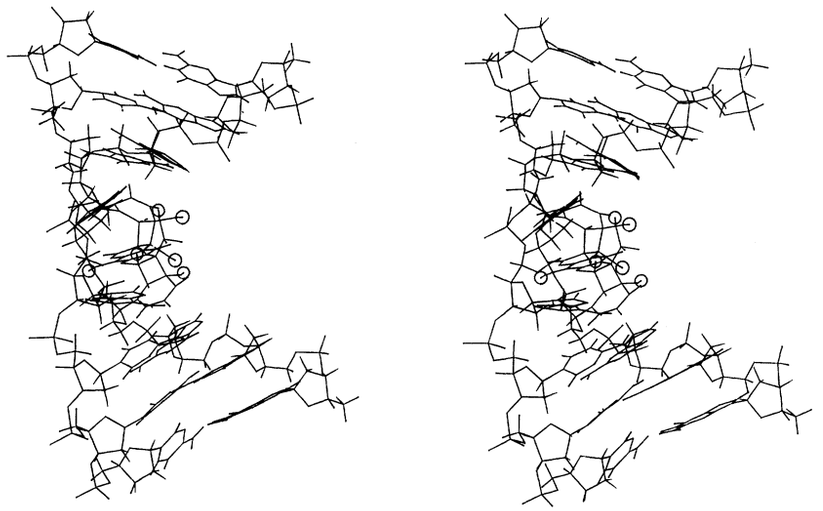

Fig. 6. Stereo picture of the NMR-derived model for DNA octamer duplex cross-linked with psoralen. All of the methyl groups and the amino group of AMT are indicated by circles.

The model-based structure presented here started as a "regularized" structure with parts of the structure about which NMR provides no direct information near the idealized B form (for example, sugar C5′, C5″, and phosphates). Because NMR provides no direct experimental distance constraints, these atoms will remain near the starting conformation during refinement unless they are influenced indirectly through van der Waals contacts or rotations of covalently attached groups. Distance geometry–derived structures (*19, 22, 23*) of this complex, which started with no assumptions about the DNA conformation except the covalently bonded structure, show proper base geometries and have approximately the same helix axis bend as the structure presented here, but with typical distortions of base pairs and backbone due to incompleteness of the bounds matrix.

The distortion of DNA structure described here provides a structural basis for understanding the results of earlier studies that showed changes in DNA sedimentation coefficient (*24*), circular dichroism (*25*), thermal denaturation behavior (*26*), and sensitivity to nucleases (*27*) and chemical reagents (*28*). Our findings are in conflict with those of Sinden and Hagerman (*29*), who concluded from gel migration of 80- to 589-base-pair fragments that were randomly reacted that psoralen cross-linked DNA is not significantly bent. NMR melting results suggest significant flexibility on one side of cross-linked DNA. Studies on the effects of cross-link flexibility on gel mobility may be needed to resolve this discrepancy.

REFERENCES AND NOTES

1. G. D. Cimino, H. B. Gamper, S. T. Isaacs, J. E. Hearst, *Annu. Rev. Biochem.* **54**, 1151 (1985).
2. J. A. Parrish, T. B. Fitzpatrick, L. Tanenbaum, M. A. Pathak, *N. Engl. J. Med.* **291**, 1207 (1974).
3. T. R. Cech and K. M. Karrer, *J. Mol. Biol.* **136**, 395 (1980); J. O. Carlson, O. Pfenninger, R. R. Sinden, J. M. Lehman, D. E. Pettijohn, *Nucleic Acids Res.* **10**, 2043 (1982); J. F. Thompson and J. E. Hearst, *Cell* **32**, 1355 (1983); B. Van Houten, H. Gamper, S. R. Holbrook, J. E. Hearst, A. Sancar, *Proc. Natl. Acad. Sci. U.S.A.* **83**, 8077 (1986).
4. S. T. Isaacs, C. J. Shen, J. E. Hearst, H. Rapoport, *Biochemistry* **16**, 1058 (1977).
5. D. Kanne, K. Straub, H. Rapoport, J. E. Hearst, *ibid.* **21**, 861 (1982).
6. D. Kanne, K. Straub, J. E. Hearst, H. Rapoport, *J. Am. Chem. Soc.* **104**, 6754 (1982).
7. H. Gamper, J. Piette, J. E. Hearst, *Photochem. Photobiol.* **40**, 29 (1984); W. Zhen, O. Buchardt, H. Nielsen, P. E. Nielsen, *Biochemistry* **25**, 6598 (1986).
8. K. Straub, D. Kanne, J. E. Hearst, H. Rapoport, *J. Am. Chem. Soc.* **103**, 2347 (1981).
9. S. Peckler *et al.*, *J. Mol. Biol.* **162**, 157 (1982).
10. S.-H. Kim *et al.*, *Cold Spring Harbor Symp. Quant. Biol.* **157**, 361 (1983).
11. D. A. Pearlman, S. R. Holbrook, D. H. Pirkle, S.-H. Kim, *Science* **227**, 1304 (1984).
12. T. Atkinson and M. Smith, in *Oligonucleotide Synthesis: A Practical Approach*, M. J. Gait, Ed. (IRL Press, 1984), pp. 35–81, Fractosil 500 Å pore was derivatized with 5′-dimethoxytrityl-*C*-succinate-3′, with a loading of 53 μmol per gram of resin. Seven cycles of detritylation, condensation, and oxidation were performed on 1.7 g of nucleoside-derivatized resin with 0.5 g per step of phosphoramidite. The completed octamer was deprotected and cleaved from the resin and then extracted and treated to remove the dimethoxytrityl protecting group. The 5′-hydroxy octanucleotide was purified by high-performance liquid chromatography (HPLC). The unmodified octamer eluted as one main peak on the HPLC with greater than 95% purity, as determined by NMR.
13. Three moles of AMT (*4*) were added per mole of double-stranded octamer, 0.5 m*M* in 30 m*M* Na_2HPO_4, *p*H 7, before irradiation. The solution was stirred under nitrogen and irradiated with 320 to 380 nm of UV light at 0°C for 15 minutes (*14*). Up to 35% of the original starting material was converted to cross-link. Total recovery of oligonucleotide from the cross-linking reaction was 85 to 95%, as determined by absorbance at 260 nm; purity was >95% after size exclusion chromatography, as determined by NMR. Because of the lower photoreactivity of cytosine with psoralen (*1, 5*), monoadducts formed at sites other than the center of this molecule would not be expected to form cross-link. All samples were handled under low light conditions. UV shadowing of a 20% polyacrylamide 1% bisacrylamide gel in 7*M* urea was used to show time dependence of AMT photoadduct formation with DNA. Samples of 1 m*M* octamer, 1.5 m*M* AMT, and 30 m*M* NaCl were stirred under nitrogen and irradiated with 320 to 380 nm UV light at 0°C for 15 minutes (*14*). After irradiation, samples were diluted with an equal amount of 8*M* urea and 1-ml aliquots were separated on a 1 cm by 40 cm P10 column with 4*M* urea, 40 m*M* NH_4COOCH_3 buffer, *p*H 7, at a flow rate of approximately 0.5 ml/min.
14. G. D. Cimino *et al.*, *Biochemistry* **25**, 3013 (1986).
15. The spectrum of unmodified octamer in D_2O was assigned with the standard sequential method [D. R. Hare, D. E. Wemmer, S.-H. Chou, G. Drobny, B. R. Reid, *J. Mol. Biol.* **171**, 319 (1983)]. All of the expected cross peaks in the aromatic proton to H1′ and H2′, H2″ sugar proton regions were observed; protons other than some H5′ and H5″ could be unambiguously assigned. The cross peak intensities at a mixing time of 100 msec suggest that there are no significant structural anomalies in this native form. Imino proton resonances were assigned with sequential one-dimensional NOEs. These resonances showed typical broadening with increasing temperature that reflect "end fraying." The spectrum was unobservably broad above 40°C.
16. J. Kemmink, R. Boelens, R. Kaptein, G. A. van der Marel, J. H. van Boom, *Eur. J. Biochem.* **162**, 37 (1987).
17. D. R. Hare and B. R. Reid, *Biochemistry* **25**, 5341 (1986).
18. J. Kemmink *et al.*, *Nucleic Acids Res.* **15**, 4645 (1987).
19. Structural calculations used the DG and DSPACE programs, Hare Research, Woodenville, WA. During the refinement we included 171 interproton distance constraints determined from 2D NOE spectra and standard hydrogen bond distances in G-C base pairs; 16 of these were between the T-AMT-T adduct and neighboring residues. Uncertainties of ±0.3 Å were assigned for distances greater than 3 Å and ±0.2 Å for distances less than 3 Å. Refinement of both embedded (distance geometry) and model-based structures was performed with a conjugate gradient minimization of an error function, which included terms for bond lengths, geminal distances, van der Waals violations, hydrogen bonds, aromatic ring planarity, and experimental distances. These had variable weights that were altered during the refinement to accelerate convergence but were equal in weight for the final minimizations.
20. In this study the helical axis was defined by least squares fitting of the first base pair of a regular duplex to the last base pair in each helical region of the model.
21. Griffith *et al.*, personal communication.
22. D. R. Hare *et al.*, *Biochemistry* **25**, 7445 (1986).
23. ———, *ibid.*, p. 7456.
24. D. T. Denhart and K. C. Kato, *J. Mol. Biol.* 77, 479 (1973).
25. T.-M. Wang and A. D. MacLaren, *Biophysik* **8**, 237 (1972).
26. Y. Shi and J. E. Hearst, *Biochemistry* **25**, 5895 (1986); F. N. Hays *et al.*, *J. Am. Chem. Soc.* **93**, 4940 (1971).
27. R. J. Legerski, H. B. Gray, Jr., D. L. Robberson, *J. Biol. Chem.* **252**, 8740 (1977).
28. N. N. Shafrnovskaya *et al.*, *Nature (London) New Biol.* **241**, 58 (1973).
29. R. R. Sinden and P. J. Hagerman, *Biochemistry* **23**, 6299 (1984).
30. G. Bodenhausen, H. Kogler, R. R. Ernst, *J. Magn. Res.* **58**, 370 (1984).
31. G. Otting, H. Widmer, G. Wagner, K. Wüthrich, *ibid.* **66**, 187 (1986).
32. P. J. Hore, *ibid.* **55**, 283 (1983).

33. We thank D. Hare, D. Koh, J. Pease, J. Hearst, and S. Holbrook for their help and assistance. Supported by grants from the National Institute of Health (GM 31616 to S.H.K.), National Science Foundation (DMB-8400952 to S.H.K.), and Department of Energy (to D.E.W. and S.H.K.). NMR instrumentation was supported by grants from URIP of Department of Energy (DE-FG05-86ER75281) and BIP of National Science Foundation (DMB-8609035).

17 August 1987; accepted 20 November 1987